# Weakly non-linear model of a piezoelectric plate in an axial flow

Miguel Piñeirua, Olivier Doaré, Sébastien Michelin

# Weakly non-linear model of a piezoelectric plate in an axial flow

**Miguel Piñeirua[a], Olivier Doaré[a], Sébastien Michelin [b]**

a. *Unité de Mécanique, ENSTA Paristech, Palaiseau, France*
b. *Ladhyx, Ecole Polytechnique, Palaiseau, France*

## Abstract :

*We present a weakly non-linear model of a piezoelctric flag immersed in an axial flow. Numerical simulations based on Galerkin projections are carried out in order to evaluate the coupling between the flapping piezo-electric flag and a purely resistive circuit intended to simulate the electric energy harvesting circuit. The numerical simulations allow to point out the relevant physical parameters governing the apparition of the flapping instability, power conversion and system's harvesting efficiency.*

## Résumé :

*Nous présentons un modèle faiblement non-linéaire d'une plaque piézoélectrique dans un écoulement axial. À l'aide d'une simulation numérique basée sur des projections de Galerkin, nous évaluons le comportement du système en flottement couplé à un circuit résistif simple. À partir de la simulation nous mettons en évidence les paramètres importants dans l'apparition de l'instabilité de flottement, la puissance récupérée ainsi que l'efficacité de récupération d'énergie du système.*

## Mots clefs : **Flutter instability ; Energy harvesting ; Piezoelectricity**

## 1 Introduction

Recent efforts in the developement of new energy harvesting methods have been focused in study of fluid-solid coupled systems that allow the conversion of the kinetic energy of flows into electrical energy [6]. Appart from the classical technologies such as wind and water turbines, other techniques involving the deformation of elastic structures under the action of fluid forces have attracted the attention of several research groups. The present study is focused on the energy harvesting from the fluttering of a piezoelectric flag in an axial flow [1].

A flexible plate in an axial flow can become unstable and develop self sustained flapping if the flow velocity exceeds a critical value. If the flapping plate is made of a piezoeletric material, the plate deformation can be transformed into electrical energy. Previous works [1, 2] have studied the fully coupled dynamics of a flexible plate covered by an infinite number of piezoelectric patches conected to simple resistive circuits.

In this work, the case of a finite number of piezoeletric patches is adressed and the dynamics of the system is modeled through a weakly non-linear model [3]. The final objective of this work is to model the system as a nonlinear electrical impedance that can be implemented in electrical simulation software, in order to test energy harvesting circuits in a more efficient manner.

## 2 Physical Model

The studied system consists of an elastic flexible plate of length $L$ and width $H$ immersed in an axial flow of both uniform density $\rho$ and velocity $U_\infty$. The plate is inextensible and clamped at its leading edge. The local orientation of the plate is noted $\theta(S,T)$, where $S$ is the curvilinear coordinate along

the streamwise direction and $T$ is time. For simplicity only the 2-D motion of the plate in the $< xy >$ plane is taken into account. A finite number $N_p$ of piezoelectric patches of length $l_p$, width $H$ and

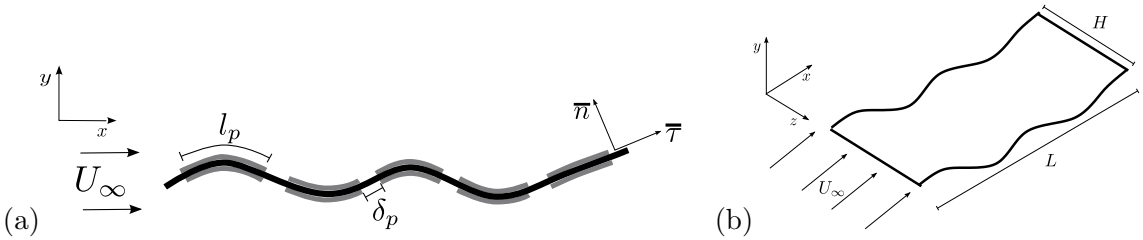


FIGURE 1 – (a) Two dimensional flapping of a flexible plate covered by pires of piezoeletric patches. (b) Flexible plate flapping in uniform axial flow.

thickness $h_p$ are fixed on both sides of the plate so that $l_p = L/N_p$. The negative electrodes of the piezo-eletric patches are shunted across the plate while their positive electrodes are connected to an external circuit. The surface density of the charge in each piezo pair is given by [1] :

$$Q_i = \frac{\chi}{l_p}[\theta]_{x_i^-}^{x_i^+} + CV_i \ , \tag{1}$$

where $V_i$ is the voltage between the positive electrodes of the $i$th piezo pair whose left and right edges are positioned at $x_i^-$ and $x_i^+$ respectively. $C$ is the equivalent capacity the piezo pair and $\chi$ is the mechanical/piezoelectrical conversion factor of the piezoelectric material. Considering that the electrodes are connected to an external resistive circuit, Ohm's law leads to :

$$\partial Q_i/\partial T + GV_i = 0, \tag{2}$$

where $G$ is the lineic conductivity of the circuit.

The voltage $V_i$ between both electrodes also generates an internal torque in the piezoeletric patches and thus on the flexible plate. The total internal torque of the bent plate will then be given by $M = B\partial\theta/\partial S - \chi\sum_i V_i F_i$, where $B$ is the flexural rigidity of the plate and piezoeletric patches assembly (see [1]) and $F_i$ is the polarization function of the $i$th patch. In the present approach, $F_i = H_s(x - x_i^-) - H_s(x - x_i^+)$, with $H_s$ the Heaviside step function.

The use of the conservation of momentum then leads to [2] :

$$\mu\frac{\partial^2\overline{X}}{\partial T^2} = \frac{\partial}{\partial S}\left(F_t\overline{\tau} - \frac{\partial}{\partial S}\left(B\frac{\partial\theta}{\partial S} - \chi\sum_i V_i F_i\right)\overline{n}\right) - P\overline{n}, \tag{3}$$

where $\overline{X}(S,T)$ $\mu$ is the local plate position and $\mu$ is the masss per unit area. $F_t$ is the internal tension in the plate that enforces inextensibility and $P$ is the pressure exerted by the surrounding fluid over the plate. Following previous works on flag flapping modeling [3], the pressure $P$ is decomposed into a resistive part $P_{resis}$ that models the drag generated by the plate as it moves inside the flow, and a reactive part $P_{reac}$ which is due to potential flow effects,

$$P = P_{reac} + P_{resis} = m_a\rho H\left(\dot{w} - (wu)' + \frac{1}{2}w^2\kappa\right) + \frac{1}{2}\rho C_d|w|w, \tag{4}$$

where $m_a$ is an added mass coefficient of the transverse section that equals $\pi/4$ for a rectangular plate. $w$ and $u$ are respectively the normal and longitudinal components of the plate's velocity relative to the fluid flow, such that $\dot{X} - U_\infty = u\overline{\tau} + w\overline{n}$.

## 2.1 Non-dimensional equations

Using $L$, $L/U_\infty$, $U_\infty\sqrt{\mu/c}$ et $U_\infty\sqrt{\mu c}$ as characteristic length, time, voltage and charge respectively, equations (1), (2) and (3) take the non-dimensional form :

$$\frac{\partial \overline{x}}{\partial t} = \frac{\partial f_t}{\partial s}\overline{\tau} - \frac{1}{U^{*2}}\frac{\partial^3\theta}{\partial s^3}\overline{n} + \frac{\alpha}{U^*}\sum_i v_i\left[\delta'(x_i^-) - \delta'(x_i^+)\right]\overline{n} - M_f p_{res} - M_f H^* m_a p_{reac}, \tag{5}$$

$$q_i = v_i + \frac{\alpha}{U^*\gamma}[\theta]_{x_i^-}^{x_i^+}, \tag{6}$$

$$\beta\frac{\partial q_i}{\partial t} + v_i = 0, \tag{7}$$

with the following non-dimmensional parameters :

$$U^* = LU_\infty\sqrt{\mu/B},\ \alpha = \frac{\chi}{\sqrt{BC}},\ M_f = \frac{\rho L}{\mu},\ H^* = \frac{H}{L},\ \gamma = \frac{l_p}{L},\ \beta = \frac{U_\infty C}{LG}.$$

The associated clamped-free boundary conditions are :

$$\text{at } s = 0,\ \ y = 0,\ \theta = 0 \tag{8}$$

$$\text{at } s = 1,\ \ f_t = \frac{\partial\theta}{\partial s} - \alpha U^* v = \frac{\partial^2\theta}{\partial s^2} - \alpha U^*\sum_i v_i(\delta(x_i^-) - \delta(x_i^+)) = 0. \tag{9}$$

Following [3], equation (5) is projected onto $x$ and $y$ in order to obtain two equations for $x(s,t)$ and $y(s,t)$ respectively. The $x$ projection is used to eliminate the tension term $F_t$ from the $y$ projection. Finally, $x$ and its derivatives are eliminated using the inextensibility condition. Keeping terms up to $O(y^3)$ one obtains a weakly non-linear equation for $y(s,t)$ :

$$L(y) + f_m(y) + \frac{1}{U^{*2}}f_B(y) - \frac{\alpha}{U^*}f_\chi(y,v) + M_f f_{res}(y) + M_f H^* m_a f_{reac}(y) = 0, \tag{10}$$

with

$$L(y) = \ddot{y} + \frac{1}{U^{*2}}y^{(4)} - \frac{\alpha}{U^*}\sum_i v_i(\delta'(x_i^-) - \delta'(x_i^+)) + M_f H^*(y'' + 2\dot{y'} + \ddot{y}),$$

$$f_m(y) = y'\int_0^s(\dot{y'}^2 + y'\ddot{y'})ds - y''\int_s^{'1}\int_0^s(\dot{y'}^2 + y'\ddot{y'})dsds',$$

$$f_B(y) = 4y'y''y''' + y'^2y^{(4)} + y''^3,$$

$$f_\chi(y,q) = \frac{1}{2}y'^2\sum_i v_i(\delta'(x_i^-) - \delta'(x_i^+)) + y'y''\sum_i v_i(\delta(x_i^-) - \delta(x_i^+)),$$

$$f_{res} = \frac{1}{2}C_D|y' + \dot{y}|(y' + \dot{y}),$$

$$f_{reac} = -\frac{1}{2}y''y'^2 + \dot{y'}y'^2 - 3y''y'\dot{y} - 2\dot{y'}y'\dot{y} - \frac{1}{2}y''\dot{y}^2 + y'\int_0^s(\dot{y'}^2 + y'\ddot{y'})ds$$

$$+ 2(y'' + \dot{y'})\int_0^s\dot{y'}y'ds - y''\int_s^1 y'(y'' + 2\dot{y'} + \ddot{y})ds.$$

A classical Galerkin decomposition is then employed : the vertical displacement $y$ is expanded on clamped-free beam eigenmodes $\phi_p(s)$,

$$y(s,t) = \sum_{p=1}^{\infty}X_p(t)\phi_p(s). \tag{11}$$

Next, equation (10) is projected on the same set of eigenmodes. After truncation to $N$ linear modes, the resulting coupled system of equations is integrated numerically using an explicit step-adaptive fourth order Runge-Kutta method.

# 3 Results

In this section results of the present model are first compared to that of reference [2]. Both models differ in two aspects : (1) a discrete number of finite length piezoelectric patches is considered here whereas a continuous distribution of infinitesimal electrodes is used in reference [2], (2) a third order weakly nonlinear approximation is used in the present paper when a fully nonlinear model is developed in reference [2]. Both models should give similar results when a large number of discrete piezoelectric patches are used and when the flapping amplitude is small.

Next, we present the impact of the number of piezoelectric patches on the linear stability threshold, the limit-cycle flapping amplitude and the harvested energy.

## 3.1 Stability Analysis

In figure 2-a we present the evolution of the stability threshold as a function of $M_f$ for different values of $\alpha$ when a large number of piezoelectric patches is used ($N_p = 100$). For small values of $M_f$, the damping induced by the electro-mechanical coupling increases the critical velocity $U_s^*$. This effect is more important as the coupling factor $\alpha$ is increased. However, for high values of $M_f$, the electro-mechanical coupling has a destabilizing effect, which was interpreted in [1] as a consequence of the existence of negative energy waves in the non-dissipative flag [5]. Our discrete model also allows to

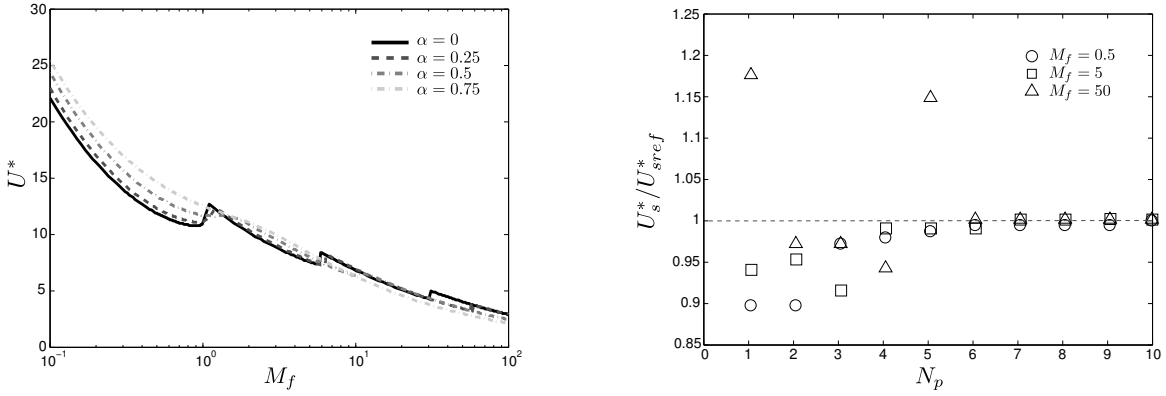


FIGURE 2 – (Left) Evolution of the stability threshold as a function of $M_f$ for different values of the coupling factor $\alpha$. (Right) Evolution of the stability threshold for three different values of $M_f$ and fixed $\alpha = 0.5$ as a function of the number of piezoelectric patches. $U_{sref}$ stands for the stability threshold speed with $Np = 100$. For both graphs $r = cst = 1$.

study the influence of the number of piezoelectric patches. As seen on figure 2-b, the stability threshold tends to a constant value when $N_p > 10$. For smaller values of $M_f$ the threshold differs.

## 3.2 Flapping regime non-linear dynamics

If the critical velocity of the stability threshold is over passed, a small perturbation of the system is enough to jump from the rest state to a flapping regime. From the linear analysis of the system the flapping amplitude should grow exponentially, however, nonlinear effects cause the saturation of the flapping amplitude leading to a permanent regime. In figure 3 we present the evolution of the flapping amplitude as a function of the non dimensional velocity $U^*$ for a flag with 100 piezoelectric patches and fixed values $M_f = 0.6$ and $\alpha = 0.5$. In the graph our results are compared to a continuous fully non linear model [2]. Near threshold both models show good agreement but for higher values of $U^*$ the weakly nonlinear model estimates flapping amplitudes that are significantly higher than those obtained by fully nonlinear model. The same differences between the two models can be observed for the energy harvesting efficiency (figure 3-b). The piezoelectric coupling factor also plays an important role in determining the flapping amplitude in the permanent regime. Because the flag tends to become stiffer as $\alpha$ is increased and because more and more energy is dissipated in the resistance, one should expect a reduction of the flapping amplitude as a function of $\alpha$. This is confirmed by the results shown

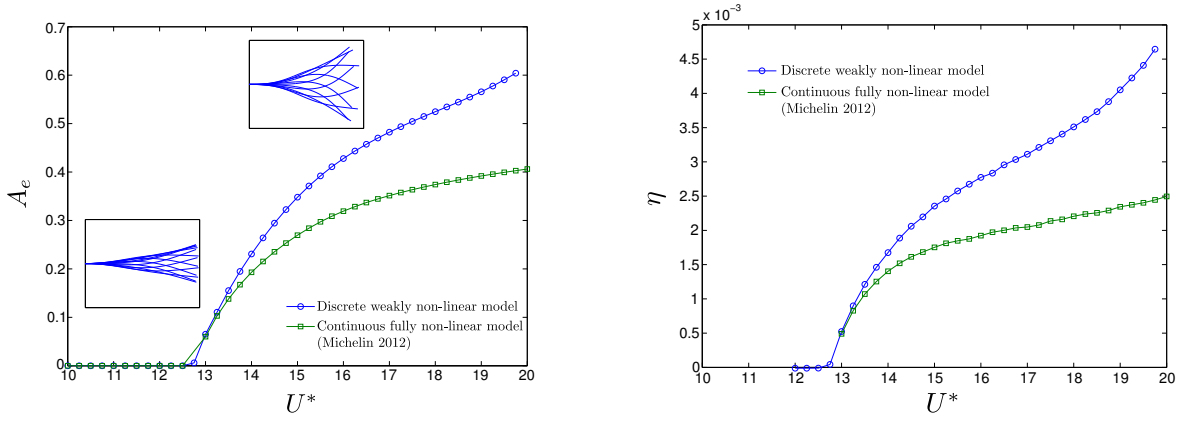


FIGURE 3 – Comparison of the the discrete weakly non-linear model with $N_p = 100$ to the continuous fully non-linear model developed by Michelin *et al.*. (Left) : non-dimensional fluttering amplitude of the trailing edge $A_e$ as a function of $U^*$. (Right) : efficiency of the energy harvesting as a function of $U^*$. Efficency is defined $\eta = P/(\rho U_\infty^3 AH)$, where $P = \sum_i^{N_p} GV_i^2$.

in figure 4-a. For flags with more than three piezoelectric patches and for fixed values of $U^* = 15$ and $M_f = 0.5$ we observe that the flapping amplitude continuously decreases as the parametes $\alpha$ is increased untill it eventually reaches a critical value for which the flag stops. This behavior is not observed in the cases $N_p = 1$ and 2, for which the amplitude increases with $\alpha$. For flags with more

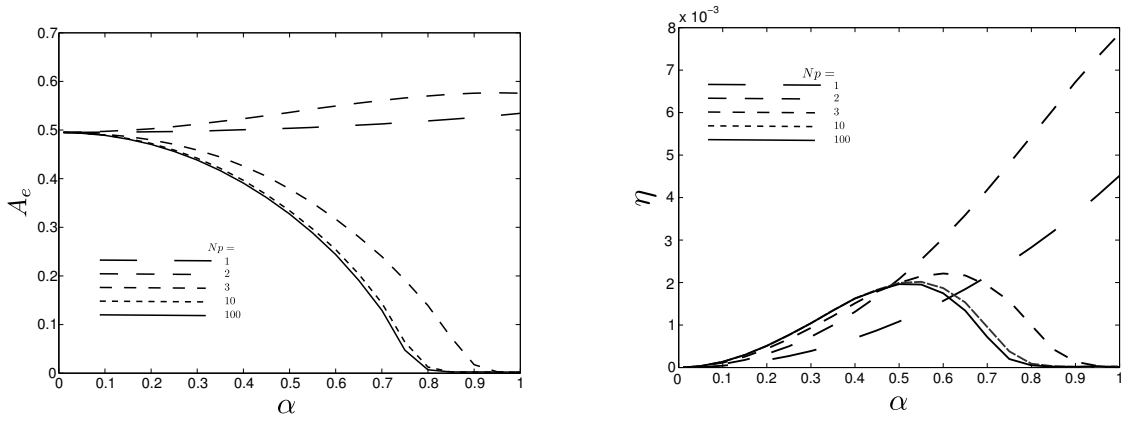


FIGURE 4 – Evolution of (Left), the trailing edge amplitude and (Right), the energy harvesting efficiency as function of the coupling coefficient $\alpha$, for $U^* = 15$, $r = 1$ and $M_f = 0.5$.

than three patches the harvesting efficiency exhibits a maximum in the range $0 < \alpha < 1$ (figure 4-b). For this particular set of parameters the optimal value of $\alpha$ is $\alpha \sim 0.55$. However, in practice $\alpha$ is restricted by the physical properties of the piezoeletric material so it is possible that this optimal value could not be reached. [1]. For this reason we must also treat prudently the efficiency of flags with one and two patches. Even if they can go have efficiencies three times greater than those of the flags with several patches, their optimal $\alpha$ value will probably be impossible to reach in real applications.

The evolution of the trailing edge amplitude and of the power and energy harvesting efficiency as a function of the non-dimensional resistance $\beta$ are shown in figure 5. For the case $\beta \ll 1$ the output electric circuit behaves like a short circuit thus there is no effect of the electric part on the flag dynamics (an equivalent case is seen when $\alpha = 0$). In the opposite case, $\beta \gg 1$, the output circuit behaves like an open circuit, so with no current flowing through the resistance no power is dissipated.

1. In a typical application involving piezoeletric materials such as PZT, $\alpha$ has been estimated in reference [1] to be around 0.3.

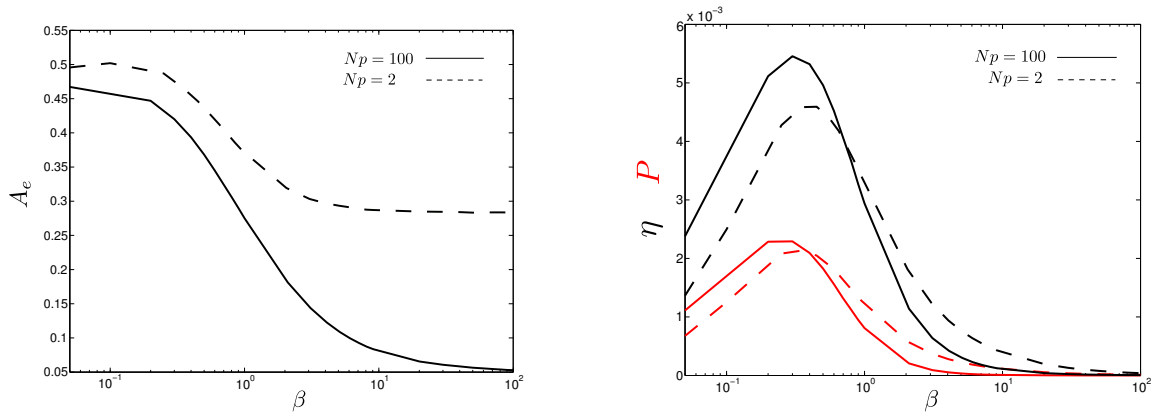


FIGURE 5 – Evolution of (left), the trailing edge amplitude and the power and (right), the energy harvesting efficiency as a function of the non-dimmensional parameter $\beta$, for $U^* = 15$, $\alpha = 0.5$ and $M_f = 1$.

Between these two extreme cases we observe a maximum in the harvesting efficiency and dissipated power for $\beta \sim 0.4$. Contrary to what is observed when $\alpha$ is varied, the dependence of the harvesting efficiency on $\beta$ has small variations when using 100 or 2 piezoelectric patches. Results obtained with 100 patches are in agreement with those presented in reference [2], where a continuous distribution of piezoelectric patches is modeled with a fully nonlinear model.

## 4 Conclusions

We have developed a weakly non linear model that describes the mechanical-electrical interactions between a fluttering flag with a discrete distribution of piezoeletric patches and a resistive circuit. Results obtained for the fluttering amplitude and harvested energy efficiency as a function of the various system's parameters are compared to previous results obtained with a fully nonlinear model that considers a continuous distribution of piezoelectric patches. For a sufficiently large number of piezo electric patches our results for the flag dynamics near the instability threshold are in good agreement with the continuous fully non linear model. However, far from threshold discrepancies between the two models are observed, mainly due to the differences of the nonlinearity order considered in each model. In the case when a small number of piezoelectric pacthes is considered, the system has a very different behavior. This effect is still to be understood. Further work shall be focused on the integration of our model as a nonlinear impedance in the developpement of electric circuit simulation software.

## Acknowledgments

This work was funded by the *Laboratoire d'Excellence* LaSIPS ("PIEZOFLAG" project).

## Références

[1] O. Doaré and S. Michelin 2011 Piezoelectric coupling in energy-harvesting fluttering flexible plates : linear stability analysis and conversion efficiency. *J. Fluid. Struct.* **27** 1357-1375

[2] S. Michelin ans O. Doare 2012 Energy harvesting efficiency of piezelectric flags in axial flows. *J. Fluid. Mech.* **714** 489-504

[3] C. Eloy, N. Kofman and L. Schouveiler 2012 The origin of hysteresis in the flag instability. *J. Fluid. Mech.* **691** 583-593

[4] M.J. Lighthill 1971 Large-amplitude elongated-body theory of fish locomotion *Proc. R. Soc. Lond. B* **179** 125-138

[5] T.B. Benjamin 1963 The threefold classification of unstable disturbances in flexible surfaces bounding inviscide flows *J. Fluid. Mech.* **16** 436-450

[6] A. Westwood 2004 Ocean power wave and tidal energy review *Refocus* **5** 50-55